

Article

Application of Bayesian Neural Network (BNN) for the Prediction of Blast-Induced Ground Vibration

Yewuhalashet Fissha ^{1,*}, Hajime Ikeda ¹, Hisatoshi Toriya ¹, Tsuyoshi Adachi ¹ and Youhei Kawamura ²

¹ Department of Geosciences, Geotechnology and Materials Engineering for Resources, Graduate School of International Resource Sciences, Akita University, Akita 0108502, Japan

² Faculty of Engineering, Hokkaido University, Sapporo 0608628, Japan

* Correspondence: d6521115@s.akita-u.ac.jp

Abstract: Rock blasting is one of the most common and cost-effective excavation techniques. However, rock blasting has various negative environmental effects, such as air overpressure, fly rock, and ground vibration. Ground vibration is the most hazardous of these inevitable impacts since it has a negative impact not only on the environment of the surrounding area but also on the human population and the rock itself. The PPV is the most critical base parameter practice for understanding, evaluating, and predicting ground vibration in terms of vibration velocity. This study aims to predict the blast-induced ground vibration of the Mikurahana quarry, using Bayesian neural network (BNN) and four machine learning techniques, namely, gradient boosting, k-neighbors, decision tree, and random forest. The proposed models were developed using eight input parameters, one output, and one hundred blasting datasets. The assessment of the suitability of one model in comparison to the others was conducted by using different performance evaluation metrics, such as R, RMSE, and MSE. Hence, this study compared the performances of the BNN model with four machine learning regression analyses, and found that the result from the BNN was superior, with a lower error: $R = 0.94$, $RMSE = 0.17$, and $MSE = 0.03$. Finally, after the evaluation of the models, SHAP was performed to describe the importance of the models' features and to avoid the black box issue.

Keywords: blasting; ground vibration; ppv; Bayesian neural network; machine learning regression



Citation: Fissha, Y.; Ikeda, H.; Toriya, H.; Adachi, T.; Kawamura, Y.

Application of Bayesian Neural Network (BNN) for the Prediction of Blast-Induced Ground Vibration. *Appl. Sci.* **2023**, *13*, 3128. <https://doi.org/10.3390/app13053128>

Academic Editors: Hao Shao and Chuanbo Cui

Received: 14 February 2023

Revised: 25 February 2023

Accepted: 27 February 2023

Published: 28 February 2023



Copyright: © 2023 by the authors. Licensee MDPI, Basel, Switzerland. This article is an open access article distributed under the terms and conditions of the Creative Commons Attribution (CC BY) license (<https://creativecommons.org/licenses/by/4.0/>).

1. Introduction

Rock blasting is one of the most common and cost-effective techniques in mining and civil engineering operations [1]. Blasting is a widely used mining technique for metal and non-metal resources, such as hard rock mining excavation and quarrying. In quarry operations, blasting requires drilling multiple rows of blast holes, with a specific spacing, burden, stemming, sub drill, face angle, bench height, and hole diameter. According to Xu et al. [2], around 30% of the energy from the whole explosion is effectively utilized to break up the rock during rock blasting, whereas the remaining energy is wasted in different ways, such as in blasting vibration, fly rock, back break, air overpressure, etc. These activities have various environmental effects and create issues for those in close proximity to the blasting zone [3]; ground vibration is one of the most severe environmental effects of blasting. This can cause damage to structures and ultimately affect peoples' lives and possessions, particularly if the buildings and structures were not designed to resist the blast's enormous destruction. According to Komadja et al.'s [4] studies, blast-induced ground vibration affects vegetation growth and can lead to deforestation. Moreover, it causes ground and slope instabilities, affecting the safety of workers during loading, drilling, and subsequent blasting activities. Additionally, people who live or work near the explosion site may experience pain and discomfort because of ground vibrations [5–7]. The release of energy that occurs during the explosion is what causes ground vibration, and the intensity of the vibration is determined by several parameters, including the amount of explosive employed, the type of rock, which is blasted, and the distance from

the source of the blast. According to Lawal et al. [7], the intensity of the blast-induced ground vibration is associated with the controllable and uncontrollable parameters of the blasting operations. The controllable blasting parameters, which include blast design parameters such as the burden, spacing, blast hole depth, diameter of the hole, stemming type and height, maximum charge weight used per delay (W), and specific charge, as well as explosive parameters such as the explosive type, detonation velocity (VoD), and powder factor, are all easy to modify, and planned based on the conditions; therefore, the blasting engineer is responsible for modifying and planning the controllable blasting parameters during the blasting design process. The uncontrolled parameters include the mechanical and physical properties of the rock, as well as the geological characteristics of the surrounding environment; the majority of uncontrolled aspects depend on the rock's natural formation.

The ground vibration movement is like a wave pattern, that travels in a circumferential direction outward from the source of the blasting. This wave motion is analogous to the ripples that travel in a circumferential direction outward when an item is thrown into a body of water and causes an impact. The peak particle velocity (PPV) is the standard baseline parameter for calculating the amount of blast-induced ground vibration, according to the rules regulating the research into blasting practice and blast-induced ground vibration. This is because the PPV is a measurement of the velocity of the most forward particles in terms of transverse (T), vertical (V), and longitudinal (L) velocities.

Various researchers have developed empirical equations to predict the intensity of blast-induced ground vibration, such as the equation that was the first meaningful PPV predictor, suggested by the United States Bureau of Mines (USBM), Duvall, and Fogleson. After a few years, different researchers modified the USBM formula, based on the scaled distance and MIC. These techniques are mathematically expressed in Equations (1)–(4). However, due to the accuracy of the predicting model, measuring the complexity of the rock mass conditions and input data parameters, and other criteria, prediction and estimation of the blasting vibration becomes a more challenging and time-consuming process. Hence, conventional empirical models are insufficient, due to the limitations of the empirical formulas.

$$\text{Duvall and Fogleson (USBM)} \quad \text{PPV} = K \left(\frac{D}{Q^{1/2}} \right)^{-b} \quad (1)$$

$$\text{Ambraseys and Hendron} \quad \text{PPV} = K \left(\frac{D}{Q^{1/3}} \right)^{-b} \quad (2)$$

$$\text{Langefors and Kihlstrom} \quad \text{PPV} = K \left(\frac{D^{1/2}}{Q^{3/4}} \right)^b \quad (3)$$

$$\text{Indian standards} \quad \text{PPV} = K \left(\frac{D}{Q^{2/3}} \right)^b \quad (4)$$

where D is the distance from the blasting face to the monitoring station (m), PPV is the peak particle velocity (mm/sec), and Q is the maximum instantaneous charge (Kg), whereas k and b are the site constants; each site has its own site constants (K and b).

To address the limitations of the conventional empirical equations, researchers over the years have used different advanced soft computing analytics to describe complicated real-world occurrences, by interrelating the characteristics that have been determined to cause such limitations. Khandelwal et al. [8], Mohamad [9], and Alipour et al. [10] predicted blast-induced ground vibration using artificial intelligence techniques, mainly artificial neural networks (ANNs). Based on the number of parameters employed to generate an ANN, their proposed models are divided into two (i.e., training and test) categories. In addition to the ANN technique, different researchers have developed a variety of artificial intelligence methods, such as the fuzzy model [11,12], linear regression, decision tree [13],

random forest [14], and deep learning, to predict and estimate blast-induced vibrations. The review study by Dumakor-Dupey et al. [15] revealed an excessive number of ML approaches being used to predict the PPV, with artificial neural network (ANN), support vector machine (SVM), and the adaptive neuro-fuzzy inference system (ANFIS) being the most frequently used algorithms (ANFIS). The interaction between the algorithms and the variables determines the efficiency of the models. Combining two or more machine learning (ML) algorithms has led to the creation of hybrid models, which improve the accuracy of stand-alone ML approaches. Nevertheless, these hybrid models provide impractical mathematical formulations, which are difficult to interpret. Table 1 summarizes the relevant research on blast-induced vibration prediction using artificial intelligence (AI) approaches in tabular form.

Table 1. Summary of selected previous studies that integrate artificial intelligence (AI) techniques for the prediction of blast-induced ground vibration. The table includes the models, input parameters, performance index, and number of datasets for each selected research.

Authors	Number of Datasets	Input Parameters	Models	Performance Index
Taheri et al. [16]	89	MCPD, D	ANN, ABC-ANN, empirical model	$R^2 = 0.92$
Arthur et al. [17]	101	MCPD, D, PF, SL B, S, AD	GPR, BPNN, MARS, ELM, MVRA	$R^2 = 0.99$ MSE = 0.09 R = 0.99 VAF = 99.17%
Khandelwal and Singh [8]	150	B, S, MCPD, HD, D V, E, Pv, BI, VoD	ANN, MVRA, empirical model	MAE = 0.24
Khandelwal [18]	128	B, S, D, CL, MCPD	ANN, empirical model	MAE = 0.18 CoD = 0.91
Bakhshandeh et al. [19]	30	S, D, T, N, MCPD	ANN, MVRA, empirical model	$R^2 = 0.977$ Error = 0.088
Saadat et al. [20]	69	D, MCPD, HD	ANN, MLR, empirical model	$R^2 = 0.95$ MSE = 0.00072
Lawal [21]	100	D, MCPD	ANN, MLR	$R^2 = 0.988$, RMSE = 2.90, VAF = 98.74 MAPE = 7.14
Zhang [22]	175	PF, T, B, S H, D, MCPD	PSO-XG Boost, empirical models	$R^2 = 0.96$ RMSE = 0.58, MAE = 0.34 VAF = 96.08
Rana et al. [23]	137	MCPD, HDM, CPH, HD, TC, D, NH, TS	ANN, MVRA, CART, empirical predictor	RMSE = 1.56 $R^2 = 0.95$
Verma and Singh [24]	127	MCPD, TC HD, B, S, T,	GA, ANN, MVRA, empirical predictor	$R^2 = 0.99$ MAPE = 0.088
Ghasemi et al. [25]	120	B, S, T, NH, MCPD, D	ANFIS-PSO, SVR	$R^2 = 0.96$ RMSE = 1.83
Iphar et al. [26]	44	MCPD, D	ANFIS, MLR	$R^2 = 0.98$ RMSE = 0.80
Saadat et al. [20]	69	MCPD, D SL, HD	ANN, empirical models	$R^2 = 0.95$ RMSE = 0.88
Peng et al. [27]	93	S, D, PF, RQD SD, B, MCPD,	ANN, ANN-PSO, ANN-GA,	R = 0.945 RMSE = 0.68
Amini et al. [28]	51	TC, D, Ve, B, S, pe	ANN	$R^2 = 0.96$
Hajihassani et al. [29]	95	B/S, T, MCPD P-wave, E, D	ANN, ICA-ANN, MLR	$R^2 = 0.97$
Faradonbeh et al. [30]	102	D, T, PF, HD, MCPD, B/S	NLMR, GEP	$R^2 = 0.87$
Vasovic et al. [31]	32	D, TC, MCPD	Empirical predictor, ANN	$R^2 = 0.9$ RMSE = 0.018

Therefore, in this study, a total of 100 datasets, from Mikurahana quarry in Japan, have been examined to develop a Bayesian neural network (BNN) prediction model and four machine learning regression techniques. Each dataset consists of different parameters such as monitoring the distance from the blasting face (D), maximum instantaneous charge (MIC), scaled distance (SD), elevation (E), blast longitudinal, blast latitude, measured longitudinal, and measured latitude. The Bayesian neural network (BNN) model, and the four machine learning techniques, are evaluated using different evaluation metrics, such as R, RMSE, and MSE. In consideration of the number of factors and assessment criteria, it was found, via the evaluation of these metrics, that they are remarkably accurate. The findings indicate that the four machine learning relationships have weak PPV estimation capabilities. However, due to its nonlinear structure, great flexibility, and low error, the BNN is much more capable of estimating the PPV compared to the other models.

The major contribution of this study is as follows: first, the study introduces a new prediction methodology using the Bayesian neural network (BNN). Second, the study introduces SHAP, and utilizes this as a feature extraction of the study; this system aids in understanding the model, the evaluation of the importance of the models' features, and in avoiding the issues of the black box. Third, new input parameters have been introduced. The overall analysis of this study with the model execution and prediction is depicted in Figure 1.

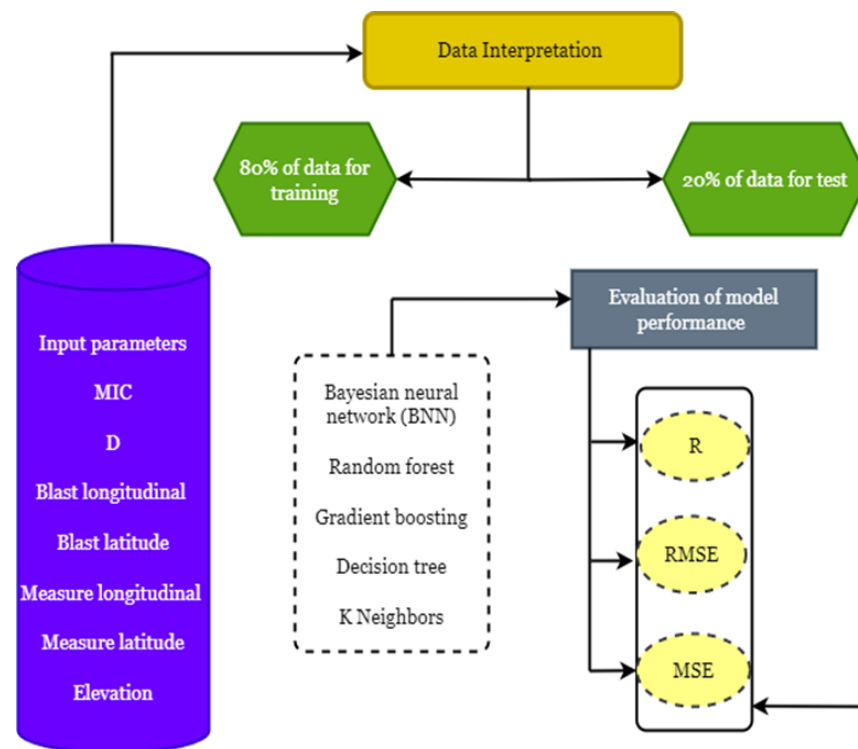


Figure 1. Flow chart of the overall analysis of the study, with model execution and prediction of PPV.

The rest of the paper is organized as follows: Section 2 provides the Materials and Methods and outlines the background on the study area, blasting vibration monitoring techniques, and details regarding the datasets and preprocessing. The proposed artificial neural network, results of the evaluation metrics, and explanation of the model's performance metrics used to assess the accuracy of the results, are presented in Section 3. Section 4 outlines the result of the BNN and the four proposed machine learning techniques. The importance of the model in the future is discussed in Section 5. The key conclusions from the research and their implications are presented in Section 6.

2. Materials and Methods

2.1. Description of the Study Area

In this study, the Mikurahana quarry site, owned and maintained by Toseki material Co., Ltd., in Hachirogata town, Akita prefecture, Japan, was selected as the target location for this research. The Mikurahana quarry can produce roughly 2000 tons of rock daily, the primary rock type being rhyolitic andesite. Figure 2 is a map that illustrates how the Mikurahana quarry is situated concerning its surroundings. As seen from the picture, there is a town, and roads that are classified as national highways, close to the quarry site. Based on this information, it was determined that the location was an appropriate target site for this research, because the inhabitants of the village live in an environment that is vulnerable to ground vibrations induced by the blasting that takes place at the Mikurahana quarry. Using the collected data on the ground vibration caused by blasting, a blasting prediction model for the quarry was developed.



Figure 2. Demonstrates (a) the Mikurahana quarry site, which is located in Hachirogata town, Akita prefecture, and (b) a map of Akita prefecture.

The blasting design parameters from the Mikurahana quarry are as follows. The diameter of vertical and horizontal holes is 65 mm, the space between vertical holes is 2–2.4 m, the length of the vertical hole is 9–9.5 m, the bench height is about 10 m, and the inclination of the vertical hole is 80° – 85° . Explosives such as ANFO, water-containing explosives, and electric detonators are the most common type of explosives used in the quarry. All the blasting design parameters of the quarry site are depicted in Figure 3.

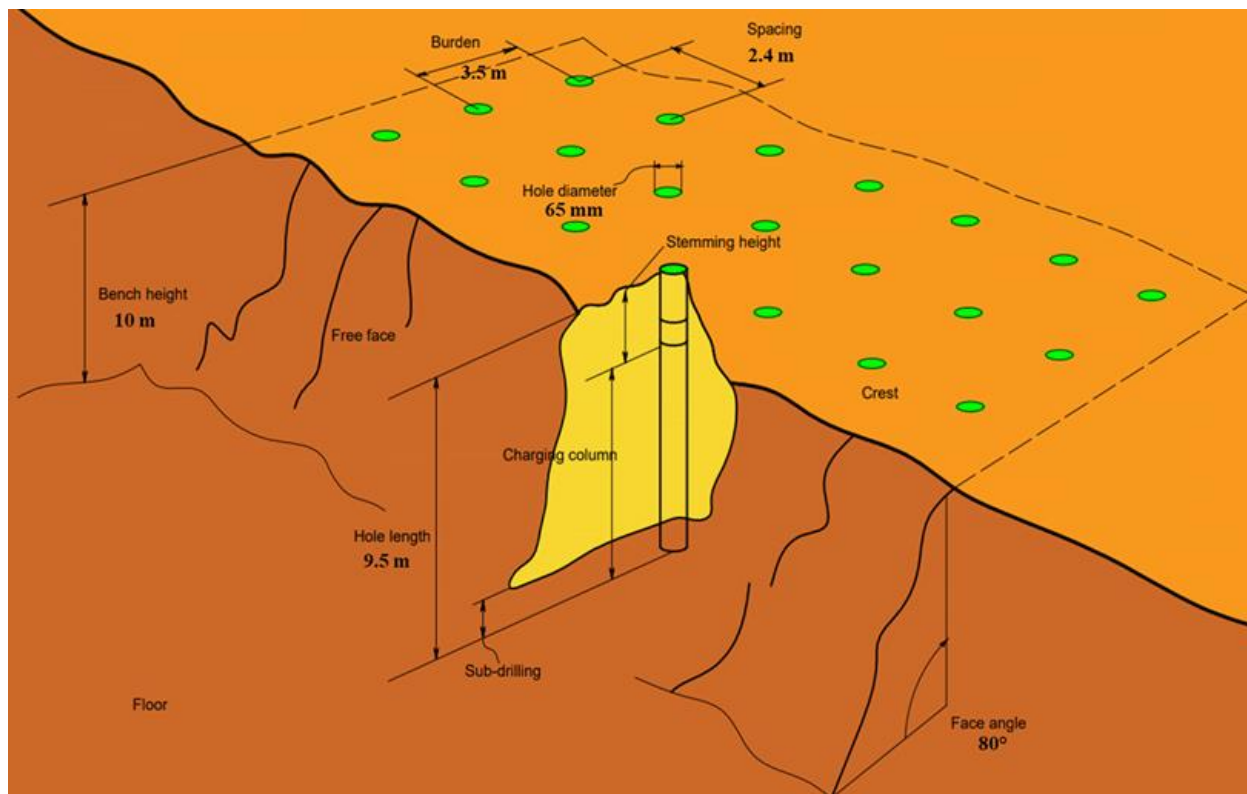


Figure 3. Blasting design of Mikurahana quarry site, with its blasting design parameters (i.e., bench height, stemming, face angle, burden, spacing, diameter of the hole, and charge column).

2.2. Blasting Vibration Monitoring at Mikurahana Quarry Site

Monitoring equipment for the blasting vibration is necessary to measure the vibration and air blast caused by quarry blasting. Locating the monitoring equipment is the first step of installation. Before doing so, the quarry management team evaluated the quarry size, blasting method, and nearby structures. After deciding on the location, we set up and calibrated the equipment, according to the manufacturer's instructions; we used a variety of vibration-measuring equipment at the Mikurahana quarry site and installed them as we had prepared. The main pieces of equipment we used were a laptop computer, seismographs, geophone, and data recorders. All the equipment is depicted in Figure 4. Seismographs monitor the frequency and amplitude of the ground vibrations induced by blasting and are used to assess whether the blast exceeds the regulation limit. On the other hand, accelerometers determine the direction and length of the vibration, by measuring the acceleration of the ground induced by the explosion. Data loggers are used to gather and store the data acquired by the seismographs and accelerometers, which may subsequently be examined and utilized to modify the blasting process, to reduce the environmental effects. Utilizing the correct technology for the monitoring of blasting vibration is crucial for maintaining the safe and effective operation of quarries.



Figure 4. Ground vibration monitoring instruments (a) laptop computer, (b) geophone, (c) data logger, and (d) seismograph.

2.3. Dataset and Pre-Processing

The ground vibration dataset consists of 100 data points. There are eight inputs: the MIC, SD, distance, elevation, blast longitudinal, blast latitude, measured longitudinal, and measured latitude, while the PPV is the output. Table 2 indicates the descriptive statistical analysis of the dataset, and Figure 5 illustrates the frequency histogram of the dataset. The dataset was split into training dataset (80% of the total dataset) and testing dataset (20% of the total dataset). Due to the variation in the dataset in Figure 5, normalization was applied, to avoid overfitting and to increase the model's learning performance. Equation (5) expresses the formula of normalization.

$$x_{normalised} = \frac{(x - x_{minimum})}{(x_{maximum} - x_{minimum})} \quad (5)$$

where x represents the initial value, $x_{minimum}$ represents the minimum value in the dataset, $x_{maximum}$ represents the highest value in the dataset, and $x_{normalized}$ represents the normalized value. Normalization is typically between 0 and 1.

Table 2. Descriptive statistics of the input and output variables.

Descriptive	MIC (kg)	Distance (m)	Elevation (m)	Blast Longitudinal	Blast Latitude	Measured Longitudinal	Measured Latitude	SD (m/kg ^{1/2})	PPV (mm/s)
Count	100	100	100	100	100	100	100	100	100
Mean	26.1	350.01	19.1	39.98	140.0	39.98	140.0763	68.64	0.62
Std	2.13	70.77	9.03	0.000709	0.00058	0.0015	0.001312	13.8	0.36
Min	23	206.64	1	39.98	140.1	39.98	140.0744	40.5	0.18
25%	24.42	296.067	15	39.98	140.07	39.98	140.0752	58.06	0.365
50%	25.5	348.6715	18	39.986	140.07	39.98	140.0763	68.3	0.53
75%	28.5	400.12	26	39.98	140.08	39.9	140.0771	78.4	0.77
Max	32.5	482.18	44	39.987	140.08	39.9	140.081	94.5	1.87

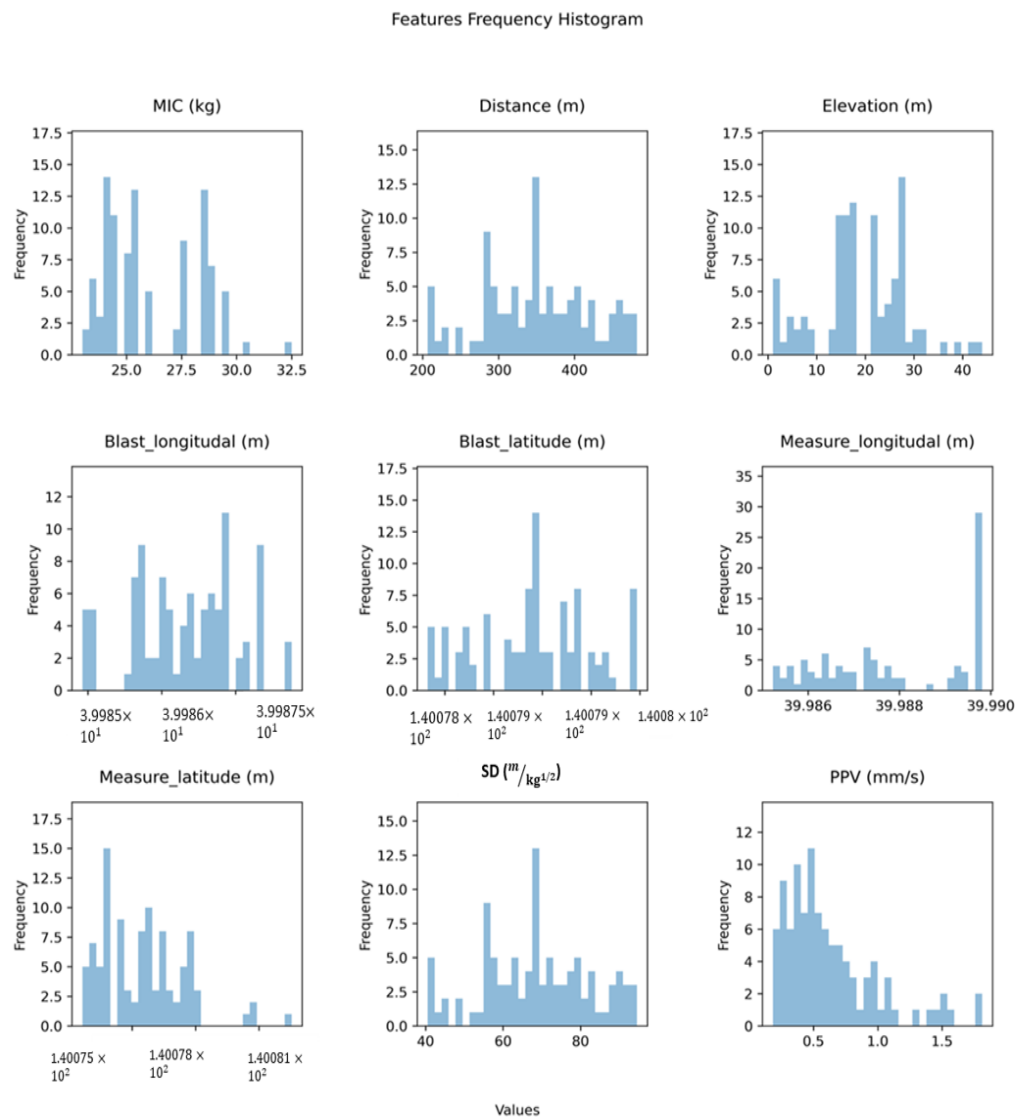


Figure 5. Frequency distribution of the ground vibration dataset.

3. Proposed Artificial Neural Network (ANN) Model

Artificial neural networks, often known as ANNs, are artificial intelligence (AI) technology capable of handling complex problems in a manner similar to that of humans. Multiple applications have used ANNs as a tool, including image recognition, audio recognition, and natural language processing [32,33].

To solve a problem, the ANN does not need prior knowledge of the relationships between the variables involved, unlike many statistical and probabilistic techniques. Similar to

nonlinear regression models, ANNs can precisely solve nonlinear regression problems; the similarity in structure between ANNs and the human brain makes this possible [22,34,35].

Some researchers, such as Moyadei and Rezaei [33], believe that the feed-forward back propagation (BPNN) algorithm is the most efficient learning technique for multilayer neural networks, among the several algorithms that may be utilized in an ANN (Figure 6). The learning process may be either unsupervised or supervised. Unsupervised is the most common approach for regression and classification problems, and it is used to predict the peak particle velocity (PPV) in this study. The ANN must be trained by analyzing many input and output patterns. The ANN then interprets the observational data into the hidden layer. First, a layer, or layers, of hidden neurons create the weights transmitted by the transfer function of the neurons in the input layer, and then the output layer performs the desired output prediction.

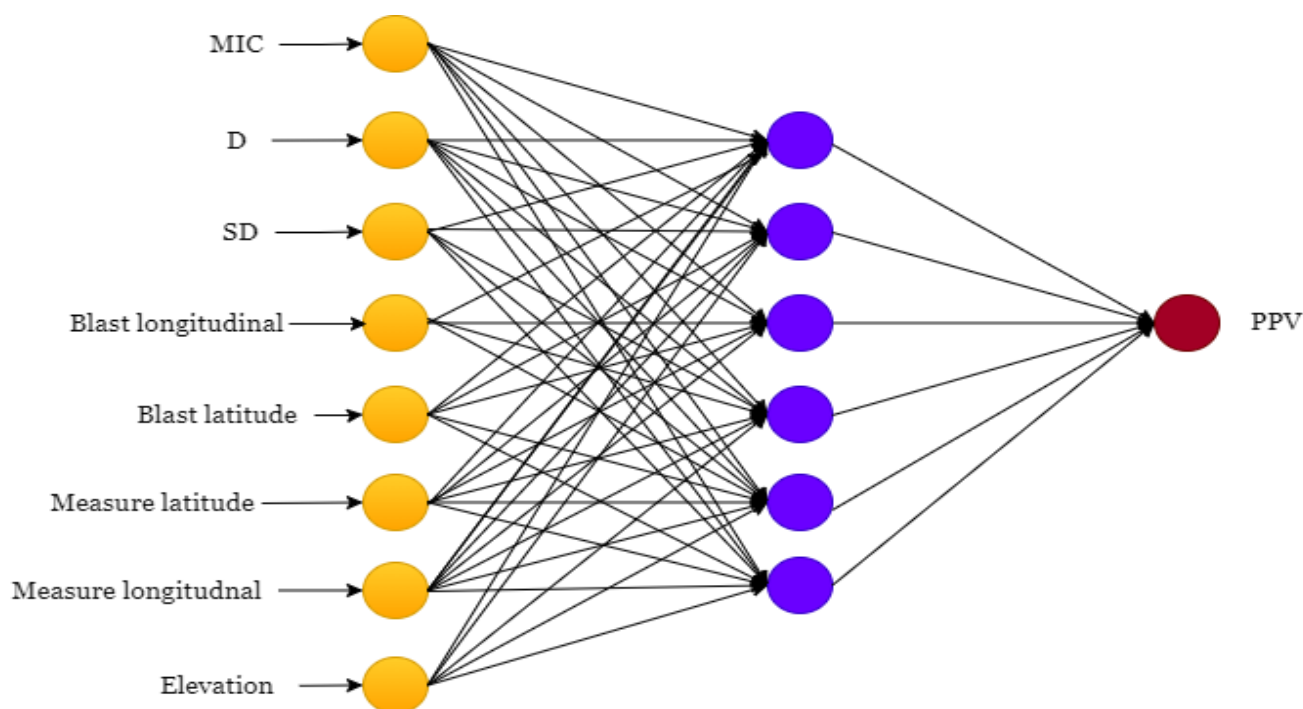


Figure 6. The architecture of a back propagation neural network (BPNN), with its three layers (i.e., input layer, hidden layer, and output layer).

3.1. Network Training

Before analyzing new input data, a network must be trained. There are a number of methods for training neural networks, but the back propagation algorithm is the most flexible and efficient. This is the most effective way for multilayer neural networks to learn. In addition, the extensive application of back propagation algorithms results from their efficiency in resolving prediction issues. Three layers are always included in feed-forward back propagation neural networks (BPNNs): input, hidden, and output. Thus, the feed-forward back propagation neural network consists of input, hidden, and output layers (BPNN). Each layer contains several neurons, the fundamental processing units, and each neuron is connected to the next layer through weights. The neurons in the input layer transmit their output to the neurons in the hidden layer. The number of input and output neurons corresponds to the input and output variables.

Training a network involves sending data from the input layer to the hidden layers, and then to the output layer (forward pass). The output is then compared to the recorded values (the “true” output). To change connection weights, the network adjusts the difference or error, and each neuron biases input–output training pairs. This procedure is repeated for each training pair in the dataset until the network error converges to a function; typically,

the root-mean-square error (RMSE), or sum of the squared errors, is used to determine the convergence (SSE).

3.1.1. Bayesian Neural Network (BNNs)

A Bayesian neural network is a form of artificial neural network (ANN) that combines the flexibility and versatility of ANNs, with the ability to handle the uncertainty of the model's parameters. It establishes the probability distribution of the model's parameters using Bayesian inference, as opposed to point estimations, unlike conventional ANNs. This enables BNNs to incorporate uncertainty into their predictions and provide more accurate results. BNNs have been implemented in a variety of applications, including image classification, natural language processing, and reinforcement learning [36].

Murat [37] explains the Bayesian framework for neural networks; his Bayesian research approach focuses on the probabilistic interpretations of network architectures. In contrast to conventional network training, in which the optimum weights are obtained by minimizing the error function, the Bayesian approach employs a probability distribution of the network weights. Therefore, the general network's prediction is based on a probability distribution. In the Bayesian concept, the network weights are random variables, and their posterior distribution may be modified according to Bayes' rule [38].

Therefore, the equation is as follows.

$$k(\omega | C, \alpha, \beta, L) = \frac{K(C | \omega, \beta, L)K(\omega | \alpha, L)}{K(C | \alpha, \beta, L)} \quad (6)$$

where the main neural network model is represented as K , the training sample is represented as C , the distribution of the weights is described as $k(\omega | \alpha, L) = \left(\frac{\alpha}{2\pi}\right)^{m/2} \exp\left\{-\frac{\alpha}{2}\omega^T\omega\right\}$, L is one of the particular ANNs, and ω represents the vector of the network with their weights. $K(\omega | \alpha, L)$ describes the main state of knowledge before the target data are collected, and $K(C | \omega, \beta, L)$ is a similar function, which is the probability of the data occurring given the weights. The posterior equation for the BNN network is stated in Equation (7).

$$Posterior = \frac{Likelihood \times prior}{Evidence} \quad (7)$$

A BNN can create probabilistic commitments for its predictions, and the distribution of the parameters it has learned from the observations. Hence, one may derive the type and form of the neural network's learned parameters from the parameter space. These two aspects make them BNNs attractive to both theorists and practitioners. Hence, due to its performance and accuracy of the as a predictive model, we have proposed a BNN in this study, to predict the blast induced ground vibration of Mikurahana quarry site, based on the eight input parameters, one output parameters and one hundred blasting datasets. The overall flow of a Bayesian neural network (BNN) is summarized in Figure 7.

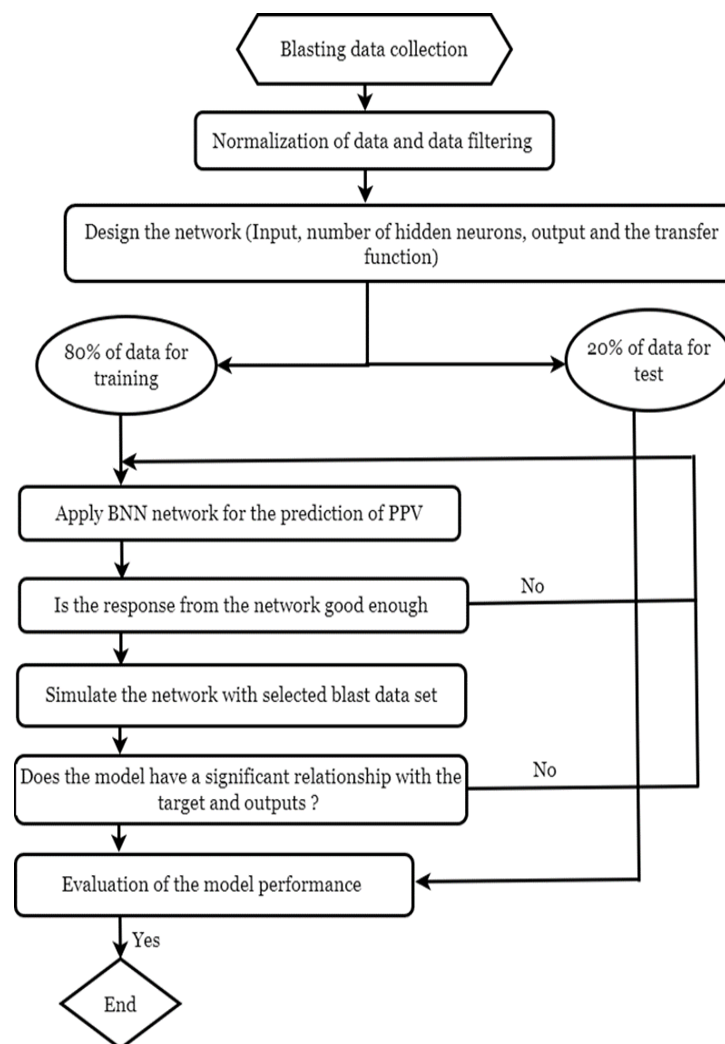


Figure 7. Flow chart of a Bayesian neural network (BNN).

3.1.2. Levenberg–Marquardt Algorithm (LMA)

Levenberg–Marquardt was developed to estimate the speed of second-order training without requiring the Hessian matrix to be calculated. Using the sum of the squares performance function, one may generate the Hessian matrix for training feed-forward networks.

Levenberg [39], in his research, optimized nonlinear least squares problems using gradient descent and an inversion of the Hessian matrix. LMA is often used to train feed-forward neural networks using back propagation. The gradient descent approach converges slower than the algorithm. Many disciplines use the Levenberg–Marquardt algorithm.

In most cases, Levenberg–Marquardt uses the approximation of the Hessian matrix shown in Equation (8).

$$X_{k+1} = x_k - [J^T J + \mu I]^{-1} J^T e \tag{8}$$

When the scalar, μ , is 0, this is Newton’s approach, using the estimated Hessian matrix. When μ is big, this becomes gradient descent, with a short step size. As soon as it is feasible, Newton’s approach should be switched to, as it is quicker and more accurate, in terms of keeping errors to a minimum. Thus, μ is dropped after each successful step (reduction in the performance function) and raised only when a tentative step will enhance the performance function. This reduces the performance function with each iteration of the algorithm.

3.1.3. Log-Sigmoid Function

The log-sigmoid function (logistic function) represents the binary outcomes in statistics and machine learning (Figure 8). The odds ratio of success to failure is its logarithm. Log-sigmoid functions convert real-valued inputs to probabilities between 0 and 1. Gradient descent optimization strategies leverage the function’s differentiability and unique derivatives in all places. Artificial neural networks employ them in the output layer of binary classification problems. The function for log-sigmoid is shown in Equation (9).

$$b = \frac{1}{1 + e^{-n}} \tag{9}$$

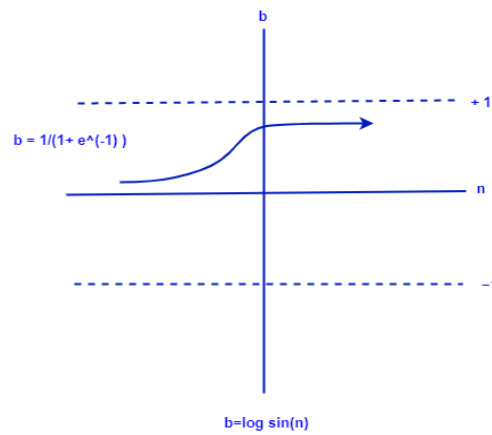


Figure 8. Log-sigmoid transfer function.

3.1.4. Linear Function

A linear system’s input–output relationship is often expressed as a polynomial equation, with the input variable acting as the independent variable and the output variable functioning as the dependent variable (Figure 9). The coefficients, commonly known as transfer function coefficients, determine the system’s behavior in the polynomial equation. Control systems, signal processing, and other branches of engineering and physics employ linear transfer functions extensively, to describe and analyze the behavior of linear systems. In addition, they are used to develop control systems capable of reaching certain performance targets. The function for the linear function is shown in Equation (10).

$$b = n \tag{10}$$

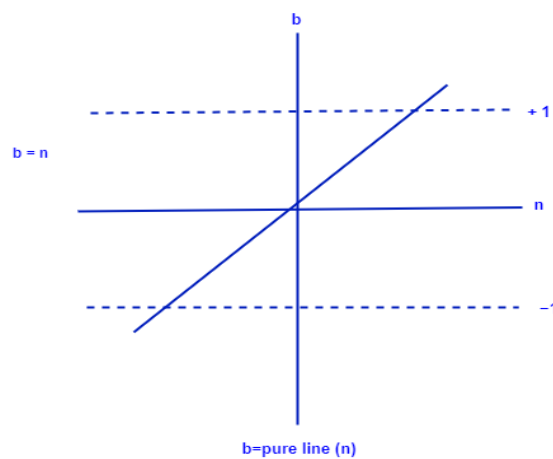


Figure 9. Linear transfer function.

3.2. Evaluation Metrics

The proposed models were evaluated using the different performance metrics; R (Pearson's correlation coefficient), RMSE (root-mean-square error), and MSE (mean squared error). The BNNs model is compared to four traditional machine learning models, to show its strength in predicting ground vibration. Sections 3.2.1–3.2.3 explain the evaluation metrics in detail.

3.2.1. Pearson's Correlation Coefficient

Measuring the degree of correlation between two or more variables is one of the most used statistical methods, with the product–moment correlation coefficient, generally known as Pearson's correlation coefficient (r), being one of the most commonly used statistics. Richard [40], in his research, described the correlation in terms of its application in a wide variety of statistics. Such as, first, establishing if two or more variables have a statistically relevant positive or negative correlation, and second, determining the level of statistical significance that may be assigned to an association.

$$r = \frac{\sum (x_i - \bar{x})(y_i - \bar{y})}{\sqrt{\sum (x_i - \bar{x})^2 \sum (y_i - \bar{y})^2}} \quad (11)$$

where r = Pearson's correlation coefficient, m = total number of observations, $y_i = y$ variable sample, \bar{y} = mean of values in y variable, \bar{x} = mean of values in x variable, and $x_i = x$ variable sample.

3.2.2. Root-Mean-Square Error

There are several techniques which can be used to evaluate the performance of a regression model, but the most frequent is to compute the root mean square error (RMSE). The root-mean-square error (RMSE) is a parameter that can be used to assess the performance of a model, by determining the amount of deviation that exists between the predicted value and the observed value [41]. The unit of the error score is the same as that of the predicted value, which is an advantage of the RMSE. The root-mean-square error (RMSE) can measure the evaluation of the matrix performance, which corresponds to the predicted value of the squared (quadratic) error or loss [42]. If y_i is the corresponding true value and \hat{y}_i is the predicted value of the i th sample, the RMSE is defined as in Equation (12).

$$\text{RMSE} = \sqrt{\frac{1}{m} \sum_{i=1}^m (y_i - \hat{y}_i)^2} \quad (12)$$

where RMSE = root-mean-square error; m = total number of observations; y_i = actual observations time series y ; and \hat{y}_i = estimated time series y .

3.2.3. Mean Squared Error (MSE)

The MSE is a common regression model evaluation approach (Equation (13)). It averages the squared differences between predicted and actual values. The mean squared error is calculated by summing the squared differences between predicted and actual values and dividing them by the number of observations. The model predicts the target variable more successfully with a lower MSE. Therefore, they were considered when evaluating the findings. Optimization- and gradient-based techniques benefit from MSEs differentiability.

$$\text{MSE} = \frac{1}{m} \sum_{i=1}^m (y_i - \hat{y}_i)^2 \quad (13)$$

where MSE = mean squared error; m = total number of observations; y_i = actual observations time series y ; and \hat{y}_i = estimated time series of y .

4. Results

The Bayesian neural network model's performance was computed utilizing the MSE, RMSE, and R evaluation metrics. Figure 10 demonstrates the regression model's actual and predicted data distribution. Figure 11 illustrates the model's learning curve with 1000 epochs; the best performance is at epoch 62, based on the mean squared error. Figure 12 indicates the model prediction error histogram. The proposed Bayesian neural network model was compared with the random forest regression, gradient boosting, decision tree, and k-neighbors regression models, to outline the performance of the BNN model. Table 3 presents the results of the comparison between the models, based on the evaluation metrics. The proposed model is superior to the traditional machine learning methods.

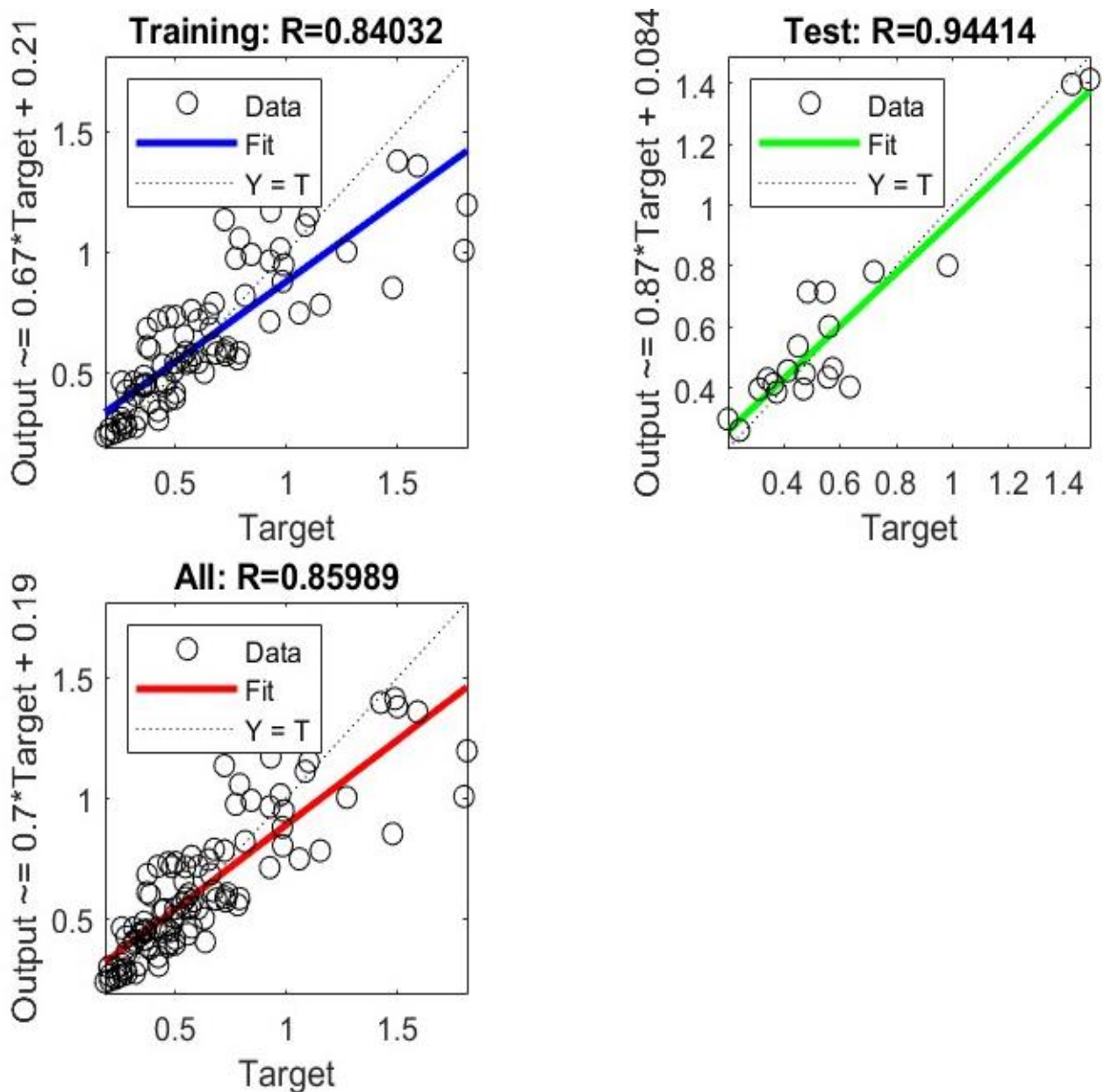


Figure 10. Actual and predicted data distribution with the fit line: the white circles are data points, and blue, green, and red lines are the best-fit lines.

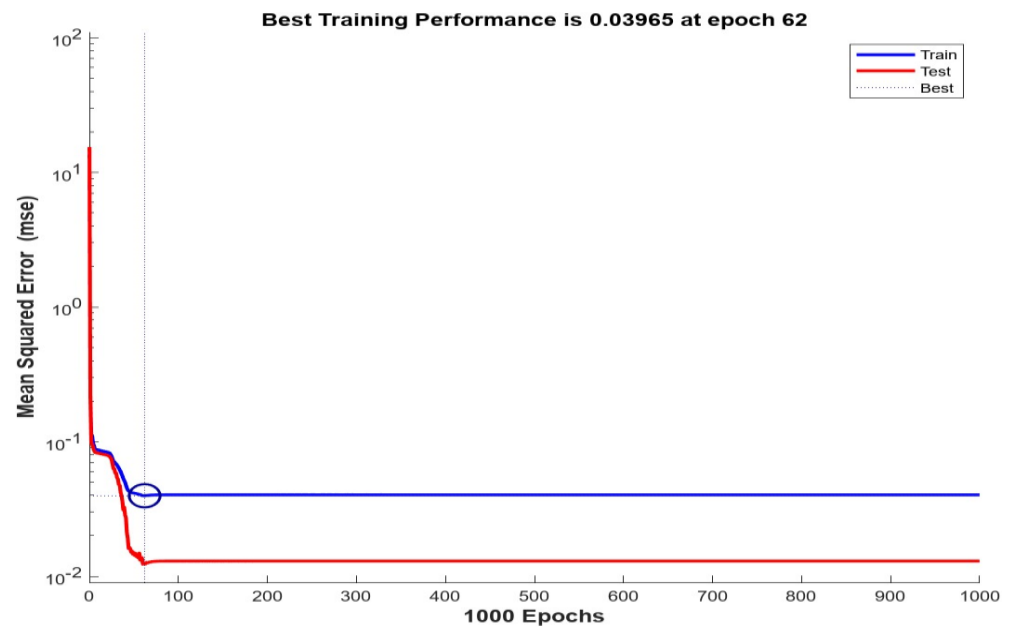


Figure 11. The BNN learning curve is as follows: the blue line is training, and the red line is the test, based on the mean squared error.

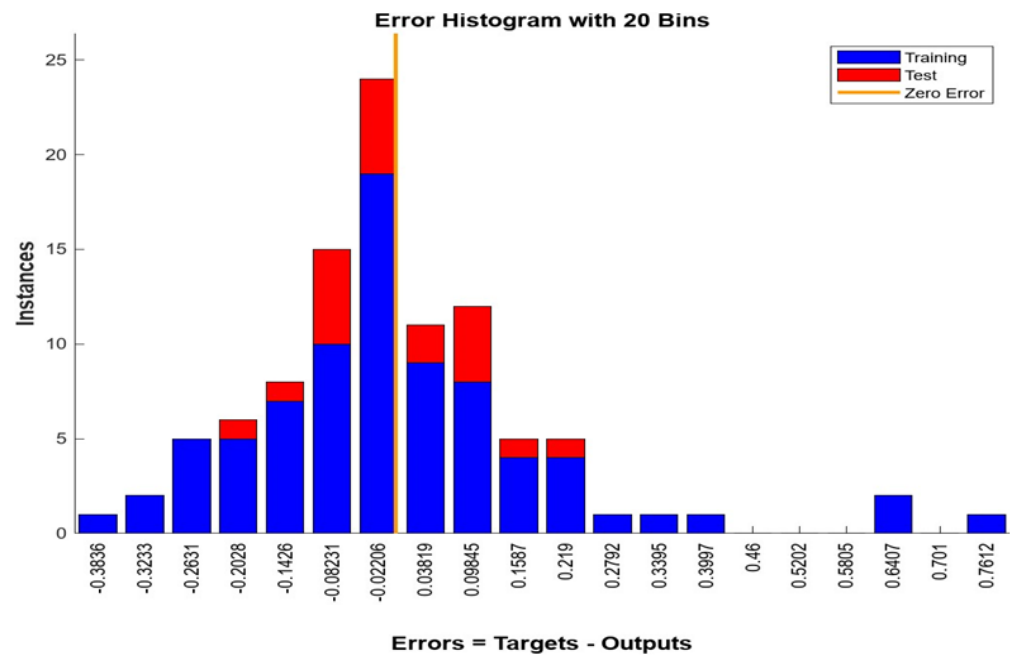


Figure 12. Proposed model prediction error histogram, the blue bars correspond to training, while the red bars refer to the test error.

Table 3. Model comparison based on the R, RMSE, and MSE evaluation metrics.

Model	R	RMSE	MSE
Bayesian neural network	94	0.17	0.03
Random forest regressor	76	0.23	0.06
Gradient boosting regressor	74	0.23	0.06
Decision tree regressor	70	0.26	0.82
k-neighbors regressor	67	0.25	0.07

Based on the results, considering the root-mean-square error, Pearson’s correlation coefficient, and the mean squared error, the proposed BNN model outperformed the four

traditional machine learning methods. The proposed BNN model obtained a Pearson's correlation coefficient of 94%, a mean squared error of 0.03, and a root-mean-square error of 0.17%. The k-NN regression model had the lowest correlation coefficient (67%), while the random forest model provided the highest correlation coefficient (76%), among the traditional machine learning models. In summary, the proposed model outperforms traditional machine learning models, making it superior in predicting ground vibration in mining blasting operations.

5. Discussion

Due to the accuracy of the predicting model, measuring the complexity of the rock mass conditions and the input data parameters, as well as the criteria, prediction, and estimation of the blasting vibration, becomes a more challenging and time-consuming process. Hence, conventional empirical models are insufficient, due to the limitations of the empirical formulas. To tackle this challenge, researchers over the years have used different machine learning techniques to describe complicated blasting vibration studies, by interrelating the characteristics that have been determined to cause such vibrations, as demonstrated in the works of Wang et al. [43], Guo et al. [44], Al Bakri et al. [45], and Chen et al. [46], who conducted different research projects using soft computing intelligence for predicting the blast vibration and understanding the wave formation associated with the blasting.

The main contribution of this research is to introduce a new prediction model, based on the Bayesian neural network (BNN), and four machine learning models (random forest, gradient boosting, decision tree, and k-nearest). Over the last few decades, researchers such as Lawal [21], Shang et al. [47], and Khandelwal [18] have used the Levenberg–Marquardt neural network for the prediction of blast-induced ground vibration. However, due to its superior accuracy, this study utilized the Bayesian neural network (BNN) rather than the Levenberg–Marquardt neural network.

In addition, this study introduced new input parameters; however, this study did not incorporate the geological features of the study area, due to limited resources, nor did we carry out experimental work related to rock properties.

Finally, after assessing the results of the models' evaluation, SHAP was performed, to understand the importance of each of the models' features and to avoid the issue of the black box. When using SHAP, it is easy to understand how each parameter contributes to a model's prediction for a particular instance. Based on the comprehensive SHAP analysis, this study shows the distance has more future importance when compared to the other input parameters. However, in this study, the spacing, diameter of the hole, burden, and bench height are not included in the study, because they each have the same value, so, based on the standard deviation, the statistical findings from the spacing, burden, bench height, hole diameter shows that there is no value, in terms of deviation, that improves the model for a better prediction, hence the BNN and four machine learning models are developed without the above listed input parameters.

Figure 13 demonstrates the importance of the input parameters for the ground vibration. Based on the SHAP analysis, this study shows the distance have the higher future importance when compared to the other input parameters.

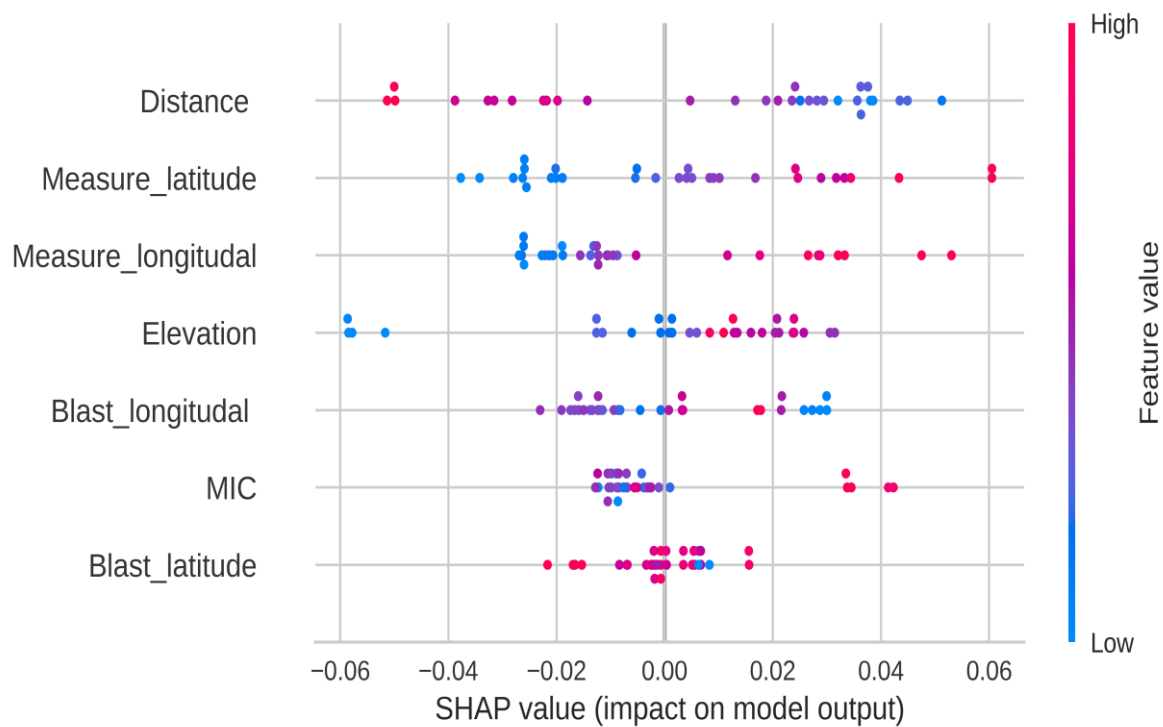


Figure 13. Feature importance of the model. Color scale: pink colors correspond to high importance of a feature, while blue colors denote low importance.

6. Conclusions

Ground vibration has a negative impact not only on the environment of the surrounding area, but also on the rock itself, and the surrounding human population. The release of energy that occurs during an explosion is what causes ground vibration; the intensity of the vibration is determined by several parameters, including the amount of explosive employed, the type of rock that is blasted, and the distance from the source of the blast. The PPV is the most important principal base parameter practice for understanding, evaluating, and predicting ground vibration, in terms of the vibration velocity. This is because the PPV is a measure of the most forward particles, in terms of the transverse (T), vertical (V), and longitudinal (L) velocities. This study aims to predict the blast-induced ground vibration of the Mikurahana quarry, using a Bayesian neural network (BNN) and four machine learning techniques, including random forest, gradient boosting, decision tree, and k-neighbors.

What follows is a few of the conclusions that can be derived from the research that was presented:

1. The proposed model was developed using eight input parameters (MIC, SD, distance, elevation, blast longitudinal, blast latitude, measured latitude, and measured longitude) and one hundred recorded blasting datasets. The data are divided into two parts: the training data (80% of the total dataset) and the test data (20% of the total dataset).
2. The assessment of one model over the other was tested by using different performance evaluation metrics, such as mean squared error (MSE), root-mean-square error (RMSE), and Pearson's correlation coefficient (R). Additionally, SHAP (Shapley additive explanation) was performed, after the evaluation of the model, to understand the feature importance of the model and avoid the issue of the black box.
3. The results obtained from the BNN model are compared with four machine learning regression analyses, and we found that the performances of the BNN model are superior to those of the traditional models, and the BNN model outperformed other models, with a lower error (RMSE = 0.17, MSE = 0.03, and R = 0.94). In consideration of the number of factors and the assessment criteria, these findings can be regarded as

remarkably accurate. For the estimation of the PPV parameters, four machine learning algorithms were evaluated. The findings indicated that these relationships have weak PPV estimation capabilities. Due to its nonlinear structure, great flexibility, and low error, a BNN is much more capable of estimating the PPV than other models.

4. By adopting the BNN technique, we can predict the PPV before a blast occurs. Adjustments may be made to the blast design so that blast disturbances are reduced, and more explosive energy will be utilized effectively and efficiently.

Author Contributions: Conceptualization, Y.F.; methodology, Y.F.; software, Y.F.; validation, Y.F.; formal analysis, Y.F.; investigation, Y.F.; resources, H.I. and T.A.; data curation, H.I.; writing—original draft preparation, Y.F.; writing—review and editing, Y.F.; visualization, Y.K. and T.A.; supervision, H.T. and T.A.; project administration, Y.K.; funding acquisition, Y.K. and H.I. All authors have read and agreed to the published version of the manuscript.

Funding: This research received no external funding.

Institutional Review Board Statement: Not applicable.

Informed Consent Statement: Not applicable.

Data Availability Statement: Not applicable.

Acknowledgments: We thank the anonymous reviewers and members of the editorial team for their comments and contributions.

Conflicts of Interest: The authors declare no conflict of interest.

Abbreviations

ABC-ANN	Artificial bee colony-artificial neural network
AD	Average depth
ANN	Artificial neural network
AMR	Angle of minimum resistance line to measured point
ANFO	Ammonium nitrate fuel oil
ANFS	Adaptive neuro fuzzy model
B	Burden
BI	Blastability index
BPNN	Back propagation neural network
CL	Charge length
CoD	Coefficient of determination
CPH	Charge per hole
D	Distance
Dh	Horizontal distance
E	Young's modulus
ED	Elevation difference
ELM	Extreme learning machine
F	Frequency
FRRL	Front row resistance line
GA	Genetic algorithm
GEP	Gene expression programming
GPR	Gaussian process regression
HD	Hole depth
HDM	Hole diameter
IC	Integrity coefficient
ICA	Imperialist competitive algorithm
MAE	Mean absolute error
MAPE	Mean absolute error percentage
MARS	Multivariate adaptive regression splines
MCPD	Maximum charge per delay
MIC	Maximum instantaneous charge

MLR	Multiple linear regression
MSE	Mean squared error
MVRA	Multivariate regression analysis
N	Number of holes
NLMR	Nonlinear multiple regression
PF	Powder factor
Pv	P-wave
PPR	Presplit penetration ratio
PPV	Peak particle velocity
PSO	Particle swarm optimization
Qtoat	Total amount of charge
R ²	Coefficient of determination
RMSE	Root-mean-square error
RQD	Rock quality designation
S	Spacing
SHAP	Shapley additive explanation
SL	Stemming length
SVR	Support vector regression
T	Stemming
TC	Total charge
TS	Tunnel cross section
VAF	Variance accounted for
VoD	Velocity of detonator
XGBoost	Extreme gradient boosting machine
ρe	Explosive density
Ve	Volume of extracted block

References

- Silva, J.; Worsley, T.; Lusk, B. Practical Assessment of Rock Damage Due to Blasting. *Int. J. Min. Sci. Technol.* **2019**, *29*, 379–385. [[CrossRef](#)]
- Xu, S.; Chen, T.; Liu, J.; Zhang, C.; Chen, Z. Blasting Vibration Control Using an Improved Artificial Neural Network in the Ashele Copper Mine. *Shock Vib.* **2021**, *2021*, 9949858. [[CrossRef](#)]
- Jahed Armaghani, D.; Hajihassani, M.; Monjezi, M.; Mohamad, E.T.; Marto, A.; Moghaddam, M.R. Application of Two Intelligent Systems in Predicting Environmental Impacts of Quarry Blasting. *Arab J. Geosci.* **2015**, *8*, 9647–9665. [[CrossRef](#)]
- Komadja, G.C.; Rana, A.; Glodji, L.A.; Anye, V.; Jadaun, G.; Onwualu, P.A.; Sawmliana, C. Assessing Ground Vibration Caused by Rock Blasting in Surface Mines Using Machine-Learning Approaches: A Comparison of CART, SVR and MARS. *Sustainability* **2022**, *14*, 11060. [[CrossRef](#)]
- Kahriman, A. Analysis of Ground Vibrations Caused by Bench Blasting at Can Open-Pit Lignite Mine in Turkey. *Environ. Geol.* **2002**, *41*, 653–661. [[CrossRef](#)]
- Giraudi, A.; Cardu, M.; Keckojevic, V. An Assessment of Blasting Vibrations: A Case Study on Quarry Operation. *Am. J. Environ. Sci.* **2009**, *5*, 468–474. [[CrossRef](#)]
- Lawal, A.I.; Idris, M.A. An Artificial Neural Network-Based Mathematical Model for the Prediction of Blast-Induced Ground Vibrations. *Int. J. Environ. Stud.* **2020**, *77*, 318–334. [[CrossRef](#)]
- Khandelwal, M.; Singh, T.N. Prediction of Blast-Induced Ground Vibration Using Artificial Neural Network. *Int. J. Rock Mech. Min. Sci.* **2009**, *46*, 1214–1222. [[CrossRef](#)]
- Mohamed, M.T. Artificial Neural Network for Prediction and Control of Blasting Vibrations in Assiut (Egypt) Limestone Quarry. *Int. J. Rock Mech. Min. Sci.* **2009**, *46*, 426–431. [[CrossRef](#)]
- Alipour, A.; Mokhtarian, M.; Sharif, J.A. Artificial Neural Network or Empirical Criteria? A Comparative Approach in Evaluating Maximum Charge per Delay in Surface Mining—Sungun Copper Mine. *J. Geol. Soc. India* **2012**, *79*, 652–658. [[CrossRef](#)]
- Azimi, Y.; Khoshrou, S.H.; Osanloo, M. Prediction of Blast Induced Ground Vibration (BIGV) of Quarry Mining Using Hybrid Genetic Algorithm Optimized Artificial Neural Network. *Measurement* **2019**, *147*, 106874. [[CrossRef](#)]
- Saeidi, O.; Torabi, S.R.; Ataei, M. Prediction of the Rock Mass Diggability Index by Using Fuzzy Clustering-Based, ANN and Multiple Regression Methods. *Rock Mech. Rock Eng.* **2014**, *47*, 717–732. [[CrossRef](#)]
- Ragam, P.; Nimaje, D.S. Evaluation and Prediction of Blast-Induced Peak Particle Velocity Using Artificial Neural Network: A Case Study. *Noise Vib. Worldw.* **2018**, *49*, 111–119. [[CrossRef](#)]
- Zhang, H.; Zhou, J.; Jahed Armaghani, D.; Tahir, M.M.; Pham, B.T.; Huynh, V.V. A Combination of Feature Selection and Random Forest Techniques to Solve a Problem Related to Blast-Induced Ground Vibration. *Appl. Sci.* **2020**, *10*, 869. [[CrossRef](#)]
- Dumakor-Dupey, N.K.; Arya, S.; Jha, A. Advances in Blast-Induced Impact Prediction—A Review of Machine Learning Applications. *Minerals* **2021**, *11*, 601. [[CrossRef](#)]

16. Taheri, K.; Hasanipanah, M.; Golzar, S.B.; Majid, M.Z.A. A Hybrid Artificial Bee Colony Algorithm-Artificial Neural Network for Forecasting the Blast-Produced Ground Vibration. *Eng. Comput.* **2017**, *33*, 689–700. [[CrossRef](#)]
17. Arthur, C.K.; Bhatwadekar, R.M.; Mohamad, E.T.; Sabri, M.M.S.; Bohra, M.; Khandelwal, M.; Kwon, S. Prediction of Blast-Induced Ground Vibration at a Limestone Quarry: An Artificial Intelligence Approach. *Appl. Sci.* **2022**, *12*, 9189. [[CrossRef](#)]
18. Khandelwal, M. Application of an Expert System for the Assessment of Blast Vibration. *Geotech. Geol. Eng.* **2012**, *30*, 205–217. [[CrossRef](#)]
19. Bakhshandeh Amnieh, H.; Mohammadi, A.; Mozdianfard, M. Predicting Peak Particle Velocity by Artificial Neural Networks and Multivariate Regression Analysis-Sarcheshmeh Copper Mine, Kerman, Iran. *J. Min. Environ.* **2013**, *4*, 125–132.
20. Saadat, M.; Khandelwal, M.; Monjezi, M. An ANN-Based Approach to Predict Blast-Induced Ground Vibration of Gol-E-Gohar Iron Ore Mine, Iran. *J. Rock Mech. Geotech. Eng.* **2014**, *6*, 67–76. [[CrossRef](#)]
21. Lawal, A.I. An Artificial Neural Network-Based Mathematical Model for the Prediction of Blast-Induced Ground Vibration in Granite Quarries in Ibadan, Oyo State, Nigeria. *Sci. Afr.* **2020**, *8*, e00413. [[CrossRef](#)]
22. Zhang, X.; Nguyen, H.; Bui, X.-N.; Tran, Q.-H.; Nguyen, D.-A.; Bui, D.T.; Moayedi, H. Novel Soft Computing Model for Predicting Blast-Induced Ground Vibration in Open-Pit Mines Based on Particle Swarm Optimization and XGBoost. *Nat. Resour. Res.* **2020**, *29*, 711–721. [[CrossRef](#)]
23. Rana, A.; Bhagat, N.K.; Jadaun, G.P.; Rukhaiyar, S.; Pain, A.; Singh, P.K. Predicting Blast-Induced Ground Vibrations in Some Indian Tunnels: A Comparison of Decision Tree, Artificial Neural Network and Multivariate Regression Methods. *Min. Metall. Explor.* **2020**, *37*, 1039–1053. [[CrossRef](#)]
24. Verma, A.K.; Singh, T.N. Intelligent Systems for Ground Vibration Measurement: A Comparative Study. *Eng. Comput.* **2011**, *27*, 225–233. [[CrossRef](#)]
25. Ghasemi, E.; Kalhori, H.; Bagherpour, R. A New Hybrid ANFIS-PSO Model for Prediction of Peak Particle Velocity Due to Bench Blasting. *Eng. Comput.* **2016**, *32*, 607–614. [[CrossRef](#)]
26. Iphar, M.; Yavuz, M.; Ak, H. Prediction of Ground Vibrations Resulting from the Blasting Operations in an Open-Pit Mine by Adaptive Neuro-Fuzzy Inference System. *Environ. Geol.* **2008**, *56*, 97–107. [[CrossRef](#)]
27. Peng, K.; Zeng, J.; Armaghani, D.J.; Hasanipanah, M.; Chen, Q. A Novel Combination of Gradient Boosted Tree and Optimized ANN Models for Forecasting Ground Vibration Due to Quarry Blasting. *Nat. Resour. Res.* **2021**, *30*, 4657–4671. [[CrossRef](#)]
28. Amini, H.; Gholami, R.; Monjezi, M.; Torabi, S.R.; Zadhesh, J. Evaluation of Flyrock Phenomenon Due to Blasting Operation by Support Vector Machine. *Neural Comput. Applic* **2012**, *21*, 2077–2085. [[CrossRef](#)]
29. Hajihassani, M.; Jahed Armaghani, D.; Marto, A.; Tonnizam Mohamad, E. Ground Vibration Prediction in Quarry Blasting through an Artificial Neural Network Optimized by Imperialist Competitive Algorithm. *Bull. Eng. Geol. Environ.* **2015**, *74*, 873–886. [[CrossRef](#)]
30. Faradonbeh, R.S.; Armaghani, D.J.; Monjezi, M.; Mohamad, E.T. Genetic Programming and Gene Expression Programming for Flyrock Assessment Due to Mine Blasting. *Int. J. Rock Mech. Min. Sci.* **2016**, *88*, 254–264. [[CrossRef](#)]
31. Vasočić, D.; Kostić, S.; Ravilić, M.; Trajković, S. Environmental Impact of Blasting at Drenovac Limestone Quarry (Serbia). *Environ. Earth Sci.* **2014**, *72*, 3915–3928. [[CrossRef](#)]
32. Tuan Hoang, A.; Nižetić, S.; Chyuan Ong, H.; Tarelko, W.; Viet Pham, V.; Hieu Le, T.; Quang Chau, M.; Phuong Nguyen, X. A Review on Application of Artificial Neural Network (ANN) for Performance and Emission Characteristics of Diesel Engine Fueled with Biodiesel-Based Fuels. *Sustain. Energy Technol. Assess.* **2021**, *47*, 101416. [[CrossRef](#)]
33. Xu, A.; Chang, H.; Xu, Y.; Li, R.; Li, X.; Zhao, Y. Applying Artificial Neural Networks (ANNs) to Solve Solid Waste-Related Issues: A Critical Review. *Waste Manag.* **2021**, *124*, 385–402. [[CrossRef](#)] [[PubMed](#)]
34. Moayedi, H.; Rezaei, A. An Artificial Neural Network Approach for Under-Reamed Piles Subjected to Uplift Forces in Dry Sand. *Neural Comput. Appl.* **2019**, *31*, 327–336. [[CrossRef](#)]
35. Bahrami, A.; Monjezi, M.; Goshtasbi, K.; Ghazvinian, A. Prediction of Rock Fragmentation Due to Blasting Using Artificial Neural Network. *Eng. Comput.* **2011**, *27*, 177–181. [[CrossRef](#)]
36. Blundell, C.; Cornebise, J.; Kavukcuoglu, K.; Wierstra, D. Weight Uncertainty in Neural Networks. In Proceedings of the 32nd International Conference on Machine Learning, Lille, France, 6–11 July 2015.
37. Kayri, M. Predictive Abilities of Bayesian Regularization and Levenberg–Marquardt Algorithms in Artificial Neural Networks: A Comparative Empirical Study on Social Data. *Math. Comput. Appl.* **2016**, *21*, 20. [[CrossRef](#)]
38. Xu, M.; Zeng, G.; Xu, X.; Huang, G.; Jiang, R.; Sun, W. Application of Bayesian Regularized BP Neural Network Model for Trend Analysis, Acidity and Chemical Composition of Precipitation in North Carolina. *Water Air Soil Pollut.* **2006**, *172*, 167–184. [[CrossRef](#)]
39. Levenberg, K. A Method for the Solution of Certain Non-Linear Problems in Least Squares. *Quart. Appl. Math.* **1944**, *2*, 164–168. [[CrossRef](#)]
40. Armstrong, R.A. Should Pearson’s Correlation Coefficient Be Avoided? *Ophthalmic Physiol. Opt.* **2019**, *39*, 316–327. [[CrossRef](#)]
41. Mei, X.; Cui, Z.; Sheng, Q.; Zhou, J.; Li, C. Application of the Improved POA-RF Model in Predicting the Strength and Energy Absorption Property of a Novel Aseismic Rubber-Concrete Material. *Materials* **2023**, *16*, 1286. [[CrossRef](#)]
42. Moustafa, S.S.R.; Abdalzaher, M.S.; Yassien, M.H.; Wang, T.; Elwekeil, M.; Hafiez, H.E.A. Development of an Optimized Regression Model to Predict Blast-Driven Ground Vibrations. *IEEE Access* **2021**, *9*, 31826–31841. [[CrossRef](#)]

43. Wang, Y.; Zheng, G.; Li, Y.; Zhang, F. Full Waveform Prediction of Blasting Vibration Using Deep Learning. *Sustainability* **2022**, *14*, 8200. [[CrossRef](#)]
44. Guo, J.; Zhang, C.; Xie, S.; Liu, Y. Research on the Prediction Model of Blasting Vibration Velocity in the Dahuangshan Mine. *Appl. Sci.* **2022**, *12*, 5849. [[CrossRef](#)]
45. Al-Bakri, A.Y.; Sazid, M. Application of Artificial Neural Network (ANN) for Prediction and Optimization of Blast-Induced Impacts. *Mining* **2021**, *1*, 315–334. [[CrossRef](#)]
46. Chen, L.; Asteris, P.G.; Tsoukalas, M.Z.; Armaghani, D.J.; Ulrikh, D.V.; Yari, M. Forecast of Airblast Vibrations Induced by Blasting Using Support Vector Regression Optimized by the Grasshopper Optimization (SVR-GO) Technique. *Appl. Sci.* **2022**, *12*, 9805. [[CrossRef](#)]
47. Shang, Y.; Nguyen, H.; Bui, X.-N.; Tran, Q.-H.; Moayed, H. A Novel Artificial Intelligence Approach to Predict Blast-Induced Ground Vibration in Open-Pit Mines Based on the Firefly Algorithm and Artificial Neural Network. *Nat. Resour. Res.* **2020**, *29*, 723–737. [[CrossRef](#)]

Disclaimer/Publisher’s Note: The statements, opinions and data contained in all publications are solely those of the individual author(s) and contributor(s) and not of MDPI and/or the editor(s). MDPI and/or the editor(s) disclaim responsibility for any injury to people or property resulting from any ideas, methods, instructions or products referred to in the content.